Tellus (2000), 52A, 225–236
Printed in UK. All rights reserved

TELLUS
ISSN 0280–6495

The variability of Atlantic–European blocking as derived from long SLP time series

By OLAF STEIN, *Meteorological Institute, University of Bonn, D-53121 Bonn, Germany*

(Manuscript received 10 August 1998; in final form 25 October 1999)

ABSTRACT

Blocking as an extreme event in European weather is addressed. A daily blocking index is applied to analyses of daily geopotential height at 500 hPa from 1949 to 1995. In order to allow for a reconstruction of these blocking time series back to 1880, daily SLP analyses are used to extract similar indices, which are optimally correlated to those based on 500 hPa. Daily indices are also determined for the geopotential height fields of 5 runs with the ECHAM3/T21 GCM, driven by monthly means of observed SST and sea ice boundaries for the years 1950–1994. These simulations differ only in their initial conditions, making it feasible to separate external variance (induced by SST and sea ice boundaries) from the atmospheric, model generated, internal variance. The index series reveal high variability both on time-scales of years to decades and interannual. Time series of spatial means show poor correlations not only between observations and simulations but also among the single runs of the model. Together with an *analysis-of-variance* (ANOVA) this leads to the conclusion, that Atlantic–European blocking is barely influenced by SST and sea ice distribution. The blocking index time series from observations is weak, yet significantly, negatively correlated to the NAO index time series favouring blocking situations during weak NAO periods.

1. Introduction

Blocking characterizes an extreme situation of European weather. In winter, when the phenomenon is most pronounced, it is most often linked with dry and cold conditions over great parts of Europe. Since a single block can persist for weeks, even a few blocking highs can determine the winter's character. There is no generally accepted definition of blocking due to the authors' different point of view. Probably the first and best known is that of Rex (1950a, b), which is strictly based on subjective criteria. He used several years of daily geopotential height at 500 hPa supposing a minimum block duration of 10 days and so marking the relevant time-scales to be established on longer time-scales than the synoptic one. Since the 1980s, numerous work has been done to investigate the dynamical and statistical features of blocking action: Austin (1980) examined the interaction between blocking and planetary waves, while Treidl et al. (1981) identified and catalogized blocking situations from more than 23 000 maps by hand.

Charney et al. (1981) compared barotropic blocking theory to blocking events from daily geopotential height observations. To use blocking criteria in a simple and objective manner for the long data series, they followed a suggestion of Dole (1978, 1986), who found a blocking situation had to be linked to a large geopotential height anomaly at 500 hPa of sufficient duration. Liu (1994), comparing the blocking criteria of Rex and Dole, yet noted that such a simple definition is not adequate.

Austin (1980) and Treidl et al. (1981) showed that a typical block is connected with a high

e-mail: ostein@uni-bonn.de

pressure area at 60°N and a low at 40°N. Using this relation Lejenäs and Økland (1983) applied geopotential height difference between 40°N and 60°N to create a longitudinal blocking index. A longitude λ was considered as blocked, if the index $I(\lambda)$ was less than zero regardless of the blocking duration.

To quantify the ability of the model in representing blocking onset and maintainance Tibaldi and Molteni (1990) made use of this index and applied a modified version to 7 years of operational analysis and forecasts of the European Centre for Medium-Range Weather Forecasts (ECMWF). In this study their index is used in a slightly modified form (in the following called TMI). The definition of blocking with the TMI is outlined in Section 9.

In recent years, blocking analysis has been extended to general circulation models (Sausen et al., 1995; Lupo et al., 1997). Tibaldi et al. (1997) applied TMI to 4 simulations of the ECHAM3 model with different horizontal resolutions and climatological or observed SST. They stated that all versions of the model underestimate the blocking frequency. From the fact that an increase of model resolution only (from T21 to T42) improves the simulation of blocking in the Atlantic–European area, while in the Pacific sector in addition more realistic SST and sea ice boundaries are necessary for a simulation improvement they supposed nonlinear internal dynamics to be mostly the cause of Atlantic–European blocking. D'Andrea et al. (1998) compared the ability of 15 general circulation models in simulating blocking for the period 1979–1988 and found large differences in blocking simulation. Compared to ECMWF analyses of the same period all models show the general tendency to underestimate both blocking frequency and the average duration of blocks. From their findings the ECHAM3 model is able to reproduce Atlantic–European blocking comparatively well.

Traditionally blocking analysis is realized with geopotential height data of the middle troposphere. Yet observations only reach back to the mid-20th century. For the purpose of climate diagnosis dealing with natural variability on timescales up to decades this is a rather short data basis. Daily sea level pressure (SLP) analyses are available since 1881 (Section 2) and are used in this study to reconstruct the TMI for the whole time basis 1881–1995 (Section 3). SLP analyses were first used for blocking studies by Lejenäs (1995), who identified blocking situations of the period 1899–1992. Following Elliot and Smith (1949) he characterized blocking by large SLP anomalies at 60°N. A blocking index obtained from SLP data is not usual since the cause of blocking is not settled at the surface and the pressure systems behave inhomogeneously. A certain justification for his proposal was given by Blackmon et al. (1979), who showed that vertical correlations between SLP and geopotential height at 500 hPa are high over the oceans. Hence Lejenäs restricted his study to the Pacific Ocean and the Atlantic Ocean including Europe up to 30°E. Comparing his results to those of Lejenäs and Økland (1983) he found a correlation of 0.7 for the time series of the frequency of blocking during winter 1960–1992.

2. Data

Daily geopotential height analyses at 500 hPa from the German Weather Service (DWD) are available on northern hemispheric gridpoints (5° × 10° lat./long.) since 1949 (Hense, 1986; Mächel, 1995). Originally manually derived, analyses since 1967 are a result of the routine objective analysis scheme of the DWD (Kaestner, 1971). In March 1989, 4-dimensional data assimilation was introduced and since 1991 the ECMWF model is used.

Daily SLP data were derived from different sources (for details see Stein and Hense, 1994). From December 1880 to November 1899 the grid point values (5° × 10° lat./long.) were interpolated from the *Hoffmeyer maps* (Hoffmeyer, 1880, 1883; Köppen, 1884). During the first geophysical year (August 1882 to August 1883) the Hoffmeyer maps were replaced by similar maps made available from the Meteorological Council, London (Anonymous, 1887; van Bebber, 1888). The interpolation was done by Hofmann and Flohn (1955).

From December 1899 to June 1939, the *Historical Weather Maps*, issued by the US Weather Service, are used (Jenne, 1975). For the period July 1939 to December 1939 data were received from the Massachsetts Institute of Technology (MIT). The dataset is often used in climate studies and was exhaustively examined

(Williams and Van Loon, 1976; Trenberth and Paolino, 1980; Jones, 1987) showing no serious data problems for the Atlantic–European area south of 70°N.

For the years 1940 to 1948, the data sources are not clear, but they obviously refer to the data available at the UK Meteorological Office (UKMO). Jones (1987) calls them *Offenbach 0001 h charts* and Glowienka (1987) historical maps of the DWD. Yet there is evidence that the origin of these charts is not Germany but the USA or the UK, since Germany was not able to carry out such extensive weather analyses in those years (H. Flohn, personal communication). From 17 February 1945 to 23 February 1945 the data miss completely. Williams and Van Loon (1976) compared the UKMO SLP data 1940–1948 with the SLP data from USA and found differences mainly in mountainous areas. Generally the years of World War I and II must be carefully interpreted because of the lack of observations especially from ships (Woodruff et al., 1987).

Since 1949, daily SLP analyses are available from the DWD. Grid point spacing and changes in the analysis scheme are identical to the geopotential height data.

Although it can be assumed that the data quality has been improved throughout the decades, homogeneity of the whole data set is considerably good. Some homogenization was achieved by interpolating all charts on the same coarse grid. Moreover blocking is a large scale phenomenon which is less affected by improvements in observation covering than, e.g., extreme low pressure events (Stein and Hense 1994).

Simulation data (500 hPa geopotential height) are from the atmospheric GCM ECHAM3 (Röckner et al., 1992) in the spectral resolution T21. This corresponds to a Gaussian grid spacing of 5.625° and is of the same order than the observation grid. Römer (1996) generated 5 runs for the years 1950 to 1994 forced by monthly means of observed SST and sea ice boundaries. The runs do not differ but for the starting conditions making it feasible to separate the simulation variance into SST induced (external) variance and fully atmospheric (internal) variance.

SST and sea ice boundary data are provided by the GISST (Global Ice and SST) dataset (Bottomley et al., 1990; Parker et al., 1994). The monthly observations of SST and sea ice boundaries were interpolated on a $5^\circ \times 5^\circ$ lat./long. grid with a linear interpolation in time to obtain daily forcing fields.

3. Reconstruction of Atlantic–European blocking

The classical approach to analyse blocking is to search for blocked situations in the geopotential height field of the mid troposphere (e.g., the 500 hPa level). Daily observations of this parameter yet do not reach back further than for the mid-20th century. In the following an attempt is made to reconstruct Atlantic–European blocking back to 1880 using the daily SLP data set described in Section 2. In the first step a modified TMI is applied to the analyses of the geopotential height field at 500 hPa from 1949 to 1995. Then similar indices for the SLP data are obtained from a modified Lejenäs (1995) index. These new indices are chosen in such a manner that the resulting time series of the occurrence of blocked days from both data sets are maximally correlated. Since both indices are vector valued data (frequency of blocking as a function of longitude), canonical correlation analysis (CCA) is used. If the explained variance of the CCA (Glahn, 1968) is high, the new "SLP blocking index" is calculated for the SLP analyses for the years 1881 to 1948. Assuming that the CCA characteristics also apply for this period TMI time series for the frequency of blocked days from 500 hPa geopotential height data can be reconstructed for SLP data for the whole period.

TMI can be used here to search for blocking situations in the geopotential height field at 500 hPa, if the different latitudinal resolution of the ECMWF data in Tibaldi and Molteni (1990) is considered (4° to 5° in the DWD dataset). So Δ must be set to $-5^\circ, 0^\circ, 5^\circ$ (see Section 9).

Following the idea of Lejenäs (1995) a "SLP blocking index" is designed as follows: a longitude λ is called blocked on a single day, if

$$p_{60^\circ\mathrm{N}}(\lambda, t) = \bar{p}_{60^\circ\mathrm{N}}(\lambda, m) + x\ \mathrm{hPa}. \qquad (1)$$

$\bar{p}_{60^\circ\mathrm{N}}$ refers to the time mean (1950–1994) of SLP at 60°N for the month m (December, January, February). x is a positive value and marks a critical deviation, which is chosen under the constraint that the CCA between both index data sets leads to a maximum explained variance. The explained variance of the CCA is defined as the ratio of the variance from the TMI data set constructed from the CCA by means of the SLP analyses to the variance of the original TMI data set. The highest explained variance of the CCA is 64% and is achieved for a critical deviation x of 8 hPa. A variety of other SLP index definitions have been examined (e.g., by introducing a minimum duration), but in all cases the correlation was smaller.

In comparison to the results of Lejenäs and Økland (1983), who used an index for the geopotential height at 500 hPa similar to the TMI, Lejenäs (1995) found a correlation of 0.7 (corresponding to an explained variance of 49%) in winter for 1960–1992. Hence the index introduced in this study is a substantial improvement if used for reconstruction.

The TMI time series can now be reconstructed back to 1880 by means of daily SLP analyses giving information about frequency and variability of Atlantic–European blocking on a time basis of 115 winters. Fig. 1 shows the % of blocked winter days (December 1880 to February 1995) depending on the longitude (a) derived directly from the SLP analyses using the "SLP blocking index" and (b) derived from the reconstruction of TMI by means of the SLP data (before 1949, for the time period 1949–1995 the original TMI is shown). A 10-year Gaussian filter is used to smooth the time series.

While Fig. 1a reveals an irregular distribution of blocking occurence in time and space, spatial distribution of blocks in Fig. 1b is in good agreement with the findings of Lejenäs and Økland (1983) and Tibaldi and Molteni (1990). It must be pointed out that the above described "SLP

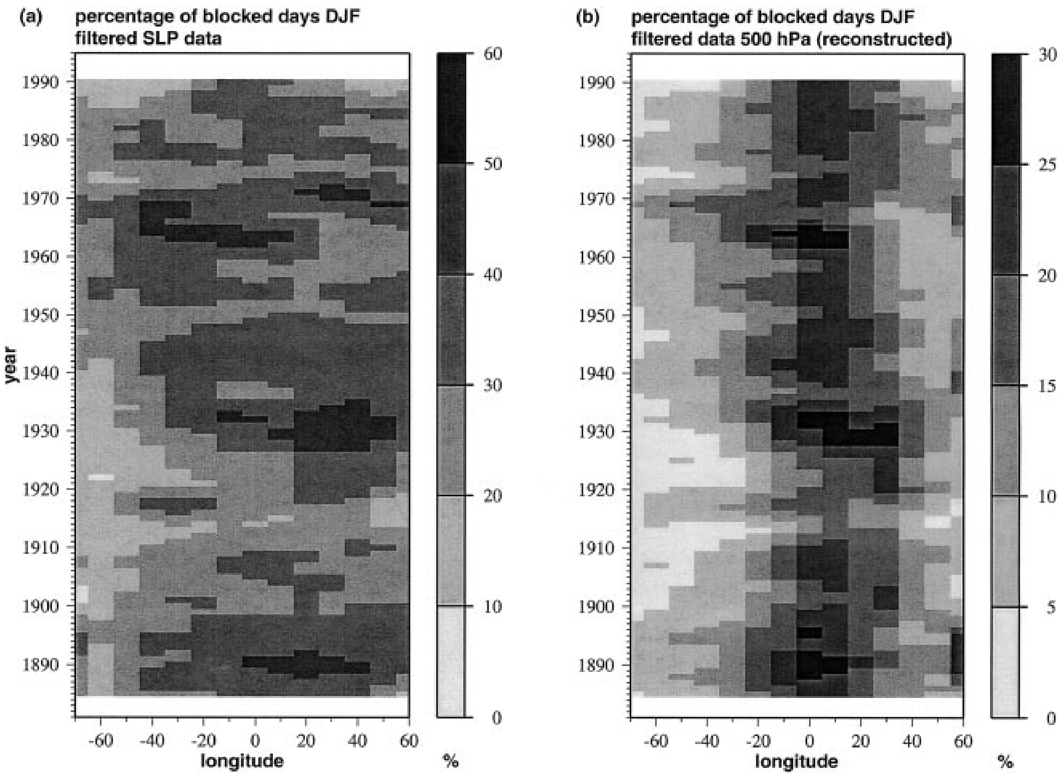

Fig. 1. Hovmöller diagram showing the % of blocked winter days ("SLP blocking index"), (a) from DWD SLP analyses December 1880 to February 1995, (b) reconstructed TMI time series back to December 1880 (before 1949, for the time period 1949–1995 the original TMI time series are shown). The data are low pass filtered with a 10-year Gaussian filter.

blocking index" is nothing but a proxy to reconstruct the TMI series in an optimal sense. The CCA defines a transfer function which extracts from the SLP index the relevant TMI structures. Therefore the interpretation has to be focussed on Fig. 1b. Maxima of blocking activity are found in the first part of the 1960s, around 1930, and around 1890. Lejenäs (1995) described the former 2 maximas and also refered to Makrogiannis et al. (1982) who found anomalous high portions of low-index situations for the period 1885–1900. Very few blocks are observed or reconstructed for the middle of the 1970s and especially in the late 1910s. Blocking activity is concentrated on the area of 20°W to 30°E.

Fig. 2 shows the 2 time series which are obtained by space averaging of the data sets from Fig. 1. In addition non-filtered time series are drawn, showing the relatively high interannual variability. The correlation between the non-filtered time series is 0.92 corresponding to an explained variance of 84%. Variability on the time scale of years to decades is also pronounced but no general trend can be detected. The non-filtered time series show a distinct minimum of blocking occurence in the late 1980s which can not be fully resolved using the low pass filtered data.

The longitudinal distribution of blocking frequency obtained by time averaging is depicted in Fig. 3. Correlation between both distributions derived from different indices is 0.81 corresponding to an explained variance of 65%. This means that the index matrices (Fig. 1) are in better temporal than spatial accordance. Maximum blocking activity (of the reconstructed TMI) is found at 10°E, where about 22% of all winter days are blocked.

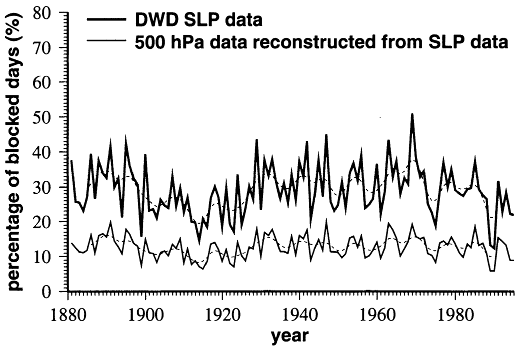

Fig. 2. Spatial means of the % of blocked winter days (DJF) December 1880 to February 1995 from DWD SLP analyses: comparison between the "SLP blocking index" time series and the TMI time series (reconstructed before 1949). A 10-year Gaussian low pass filter is applied to the dotted curves.

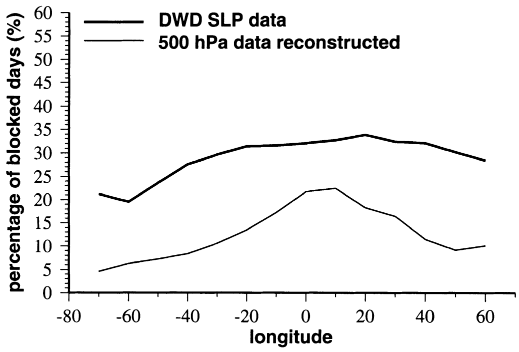

Fig. 3. As Fig. 2, but longitudinal distributions of temporal means.

4. Reconstruction quality control

An estimation of the reconstruction error can be made by cross-validating the TMI time series constructed from the CCA by means of the SLP analyses (Efron and Tibshirani, 1993). The time interval 1950–1994 was used as the time basis common to both datasets. The cross-validation estimator of the prediction error is then used to create the Brier skill score

$$B_{FCP} = 1 - \frac{S_{FP}^2}{S_{CP}^2}, \tag{2}$$

where F stands for the forecast (or reconstruction), C for the climatology, and P for the predictand (the above TMI) and S^2 is the mean squared error.

In connection with the cross-validation technique the Brier skill score is a measure of the skill of the specification model (here the reconstruction model) and should be one for a perfect reconstruction. If the reconstruction is verified over time at a fixed location the mean squared error S_{FP}^2 is given by the time mean of the squared anomalies:

$$S_{FP}^2 = \overline{(F - P)^2}. \tag{3}$$

If the reconstruction is verified across space at a fixed time (t) the mean squared error is given by:

$$S_{FP}^2 = \langle (F_t' - P_t')^2 \rangle, \quad (4)$$

$$F_t' = F_t - C, \quad (5)$$

$$P_t' = P_t - C, \quad (6)$$

where $\langle\ \rangle$ represents the spatial mean and $'$ indicate the anomalies.

Furthermore, the Murphy–Epstein decomposition of the Brier skill score is carried out (Von Storch and Zwiers, 1998), which may be expressed as:

$$B_{FCP} = \frac{A^2 - B^2 - C^2 + D^2}{1 + D^2}, \quad (7)$$

where

$$A^2 = \rho_{FP}^2, \quad (8)$$

$$B^2 = \left(\rho_{FP} - \frac{\sigma_{F'}}{\sigma_{P'}}\right)^2 = \left((b-1) - \frac{\sigma_{F'}}{\sigma_{P'}}\right)^2, \quad (9)$$

$$C^2 = \left(\frac{\overline{P'} - \overline{F'}}{\sigma_{P'}}\right)^2, \quad (10)$$

$$D^2 = \left(\frac{\overline{P'}}{\sigma_{P'}}\right)^2, \quad (11)$$

$$b = \frac{\sigma_{P'}}{\sigma_{F'}} \rho_{FP}. \quad (12)$$

The first term A^2 is the squared correlation coefficient ρ_{FP} and measures the phase error of the reconstruction. B^2 is a measure of the amplitude error such that B^2 is one and b is zero for a perfect reconstruction. C^2 is a measure for the systematic error and is greater than zero if there is any bias. In general, C^2 should be small in relation to the normalization D^2.

The cross-validated estimation of the prediction error as well as the skill score and the terms of the Murphy–Epstein decomposition are presented in Fig. 4. The results are shown as verifications of the TMI reconstruction in time and space, respectively. Values of the prediction error generally are in the order of 10 to 20% of the index % values except for single winters (1965/66, 1979/80) and for blocking events at 60°E. The latter result suggests that the assumptions leading to the blocking index are not relevant for this region. Therefore, this longitude will not be discussed further. The Brier skill score of the reconstruction is mostly larger than 0.5 indicating a better than climatology reconstruction. The term A^2 of the Murphy–Epstein decomposition corresponds to correlation coefficients of more than 0.8 except for the years 1950/51, 1959/60, and 1965/66 where the reconstruction leads to considerable phase errors. The amplitude errors must be analysed more carefully. There are several years (mainly before 1980) in which the term B^2 is high coinciding with a low b implying a substantial amplitude error for these years. While in most cases the prediction error is due to both the phase and amplitude error, the prediction error in 1965/66 is almost completely an amplitude error. Considering the dependance on longitude both phase and amplitude error are smallest near the region of maximum blocking occurence. The terms C^2 and D^2 (not shown) are extremely small implying there is almost no bias produced by the reconstruction.

Summarizing the above findings a reasonable TMI blocking reconstruction using SLP analyses is possible with an error of about 10 to 20% of the original TMI frequency % values.

5. Comparison with model simulations

Blocking situations substantially influence the weather and modify atmospheric flow patterns over large areas of the Northern Hemisphere. Forecasts as well as climate models should be able to simulate the frequency and position of blocks realistically. In the following, the modified TMI (sector 3) is applied to 5 runs with the atmospheric GCM ECHAM3/T21, which are driven by monthly means of observed SST and sea ice boundaries for the years 1950–1994 (Römer, 1996). The simulated data were interpolated on a 5° × 10° lat./long. grid before use. Fig. 5 shows the % of blocked days in the whole area (70°W–60°E) for the winter months (DJF) 1950 to 1994 in comparison to the DWD geopotential height analyses. For reasons of simplicity, only the ensemble mean of the 5 runs is plotted, the shaded area marks the range between the simulations. It is striking that the DWD analyses reveal distinctly more blocks than the simulations. Indeed the modelled blocking frequency is only about half of the analysed values. This is likely to be a fundamental problem of the spatial resolution of climate models. Boer et al. (1992) compared 14 atmospheric GCM and found an increasing meridional

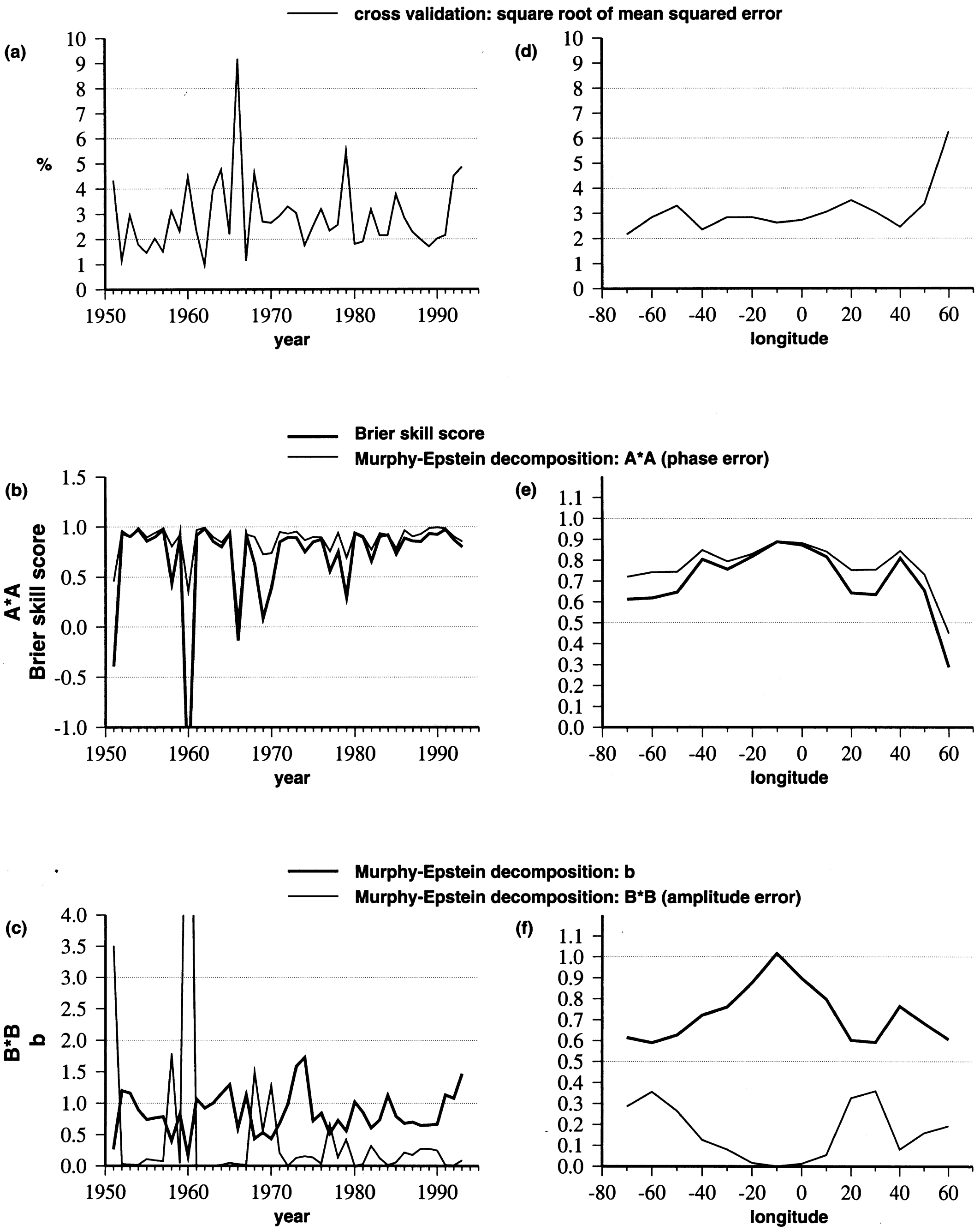

Fig. 4. Murphy–Epstein decomposition of the Brier skill score produced by the cross-validated prediction error. (a)–(c): verification in time. (a) Square root of the cross-validated mean squared prediction error of the TMI reconstruction. (b) Brier skill score and term A^2 of the Murphy–Epstein decomposition. (c) Term B^2 and b of the Murphy–Epstein decomposition. (d)–(f) As in (a)–(c) but verification in space.

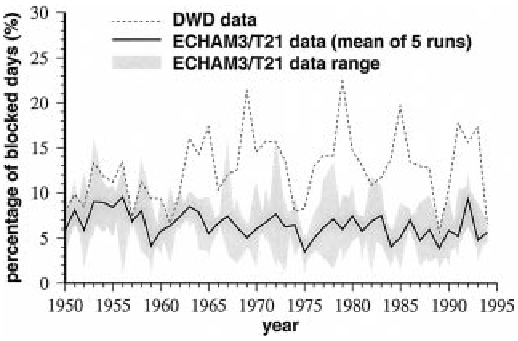

Fig. 5. Spatial means of the % of blocked winter days (DJF) January 1950 to December 1994 from 500 hPa geopotential height data: comparison between DWD analyses and 5 runs with the ECHAM3/T21 model.

circulation for an increasing horizontal resolution. Tibaldi et al. (1997) analysed blocking in a 10-year ECHAM3 GAGO (*Global Atmosphere/Global Ocean*) run and found far more realistic blocking frequencies in the Atlantic–European sector if the horizontal resolution was increased from T21 to T42.

The longitudinal distribution of blocking frequency is plotted in Fig. 6 on the basis of the 40 winters common to both the DWD and the ECHAM3 data. Again the analyses show far more blocks than the simulations. The maximum of blocking activity is shifted about 10° to the east for the simulations (see also D'Andrea et al., 1998). Variance between the runs is comparatively small.

The interannual variability in all time series is high and correlations are poor — both between DWD analyses and model simulations and from run to run (not shown). This indicates that the frequency of Atlantic–European blocking in winter is barely influenced by variations of SST and sea ice conditions. To further elucidate this suggestion an *analysis-of-variance* (ANOVA) was carried out. With the help of this statistical method the total variance of a variable in time and realization can be split into an internal ("chaotic") and an external (forced by SST an sea ice covering) portion (Rowell et al., 1995). The external variance determined by this factor reaches only about 2% of the whole variance and is not significant. Hence winter time Atlantic–European blocking seems to be more determined by the internal variability of the atmosphere which is in turn governed by nonlinear processes (Frederiksen, 1986).

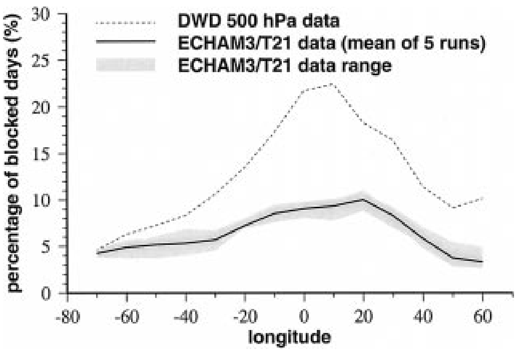

Fig. 6. As Fig. 4, but longitudinal distributions of temporal means.

6. Connection with the NAO

The North Atlantic Oscillation (NAO) is known as a synchronous northward (southward) shifting of the Icelandic Low and the Azores High together with a strengthening (weakening) of the pressure centers. This pressure see saw which was first described by Defant (1924) is found all over the year, but is most pronounced in winter, when it explains more than one third of the SLP variance in this area (Cayan, 1992). It is common practice that a NAO index is established by building pressure differences between normalized pressure anomalies of Ponta Delgadas (Azores) and Akureyri (Iceland). This index was first introduced by Walker (1924) and Walker and Bliss (1932). In this study the NAO index is defined alternatively as the first EOF of the correlation matrix from the 4 time series consisting of the position and the central pressure of Icelandic Low and Azores High (Glowienka, 1985; Glowienka-Hense, 1987).

High NAO index situations are linked with a strong pressure gradient between Icelandic Low and Azores High and hence with zonal circulation while meridional circulation patterns are favoured during low index situations. As blocking is part of a meandering, meridional circulation type over the northern hemisphere, it can be assumed that there is a negative correlation between any blocking index and the NAO index, at least in the winter months.

Correlation of the TMI and NAO index time series for winter (December to February) 1880/81 to 1994/95 shows a correlation coefficient of −0.42

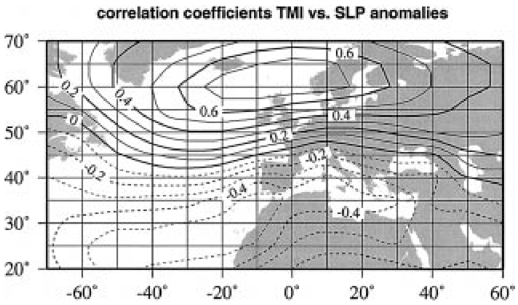

Fig. 7. Correlation map resulting from correlation of TMI and SLP anomalies time series on gridpoints DJF 1880/81 to 1994/95. The contour interval is 0.1.

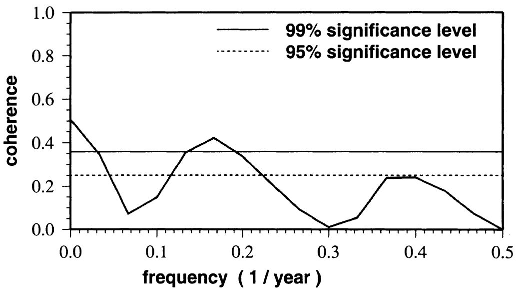

Fig. 8. Cross-spectral analysis: coherence of the TMI blocking time series and the NAO index time series for winter (DJF) 1880/81 to 1993/94.

with a 99% confidence interval of (−0.60, −0.21) and is thus relatively weak, but nevertheless significant. This supports the assumption that blocking activity intensifies during weak NAO episodes and vice versa. Correlating the TMI time series with the time series of SLP anomalies on each gridpoint results in a correlation map which is similar to the NAO pattern (Fig. 7). The maximal correlation is achieved for 10°W, 60°N with a positive correlation coefficient of 0.79.

A cross-spectral analysis of the TMI and NAO time series (Fig. 8) reveals a significant coherence on the 99% significance level with a phase shift of 180° for periods from 5 to 8 years (maximum coherence at a period of about 6 years: 0.42). This means linkage between blocking occurence and NAO takes place favourably on these time-scales.

7. Conclusion

A longitudinal blocking index basing on daily SLP gridpoint data in the Atlantic–European area was introduced by means of a canonical correlation analysis with a TMI data set from observed geopotential height analyses of the 500 hPa level for 1949 to 1995. These new index time series could then be successfully reconstructed back to 1880 leading to the longest estimate of wintertime Atlantic–European blocking occurence known yet. Maxima of blocking activity are found in the first half of the 1960s, around 1930, and around 1890. Few blocking episodes occur in the middle of the 1970s and in the late 1910s. Blocking activity is concentrated on longitudes from 20°W to 30°E. The interannual variability as well as the variability on time-scales of years to decades is high. The reconstruction error was assessed by computing the Murphy–Epstein decomposition of the skill score produced by cross-validation. Both the phase and amplitude error are small except for single years and at 60°E. No bias is generated from the reconstruction. A reasonable reconstruction of blocking frequency using SLP data is possible with an error of 10 to 20% of the original (TMI) % values.

TMI was also applied to simulations of the geopotential height field with the ECHAM3/T21 atmospheric GCM. 5 runs driven by monthly means of observed SST and sea ice conditions were analysed in comparison to the observational data. In the model simulations only about half of the number of blocked days were counted, while spatial distributions coincide well. Time series of spatial means show low correlations between simulations and analyses as well as from run to run. An ANOVA led to an external variance portion (induced by SST and sea ice variations) of only 2% of the whole variance. These facts lead to the conclusion that blocking activity is hardly influenced by SST and sea ice boundaries. The phenomenon is obviously governed by the internal variability of the atmosphere generated by nonlinear processes.

The spatial mean of the reconstructed blocking index time series is weakly, but sigificantly, negatively correlated with the NAO index time series. The correlation map resulting from correlating TMI with SLP anomalies on gridpoints resembles the NAO pattern. Blocking situations are favoured during weak NAO episodes, when pressure gradients are weak and circulation types are meridional. A cross-spectral analysis of the 2 time series reveals that the dominant time scales of coherence are found in the periods from 5 to 8 years.

8. Acknowledgements

My special thanks go to Andreas Hense for suggesting the study of blocking climatology and for providing his statistical background knowledge to me. I would like to thank Prof. Heinz-Dieter Schilling (died in 1997) and Prof. Helmut Kraus for helpful comments and discussions on the theme. This work was sponsored by the German Bundesministerium für Bildung, Wissenschaft, Forschung und Technologie under Contract 07 VKV 01/1. Suggestions of the 2 anonymous reviewers helped to improve the manuscript.

9. Appendix A

Blocking definition with the TMI

The definition of blocking from daily geopotential height fields used in this study has been set up by Tibaldi and Molteni (1990) who themselves used a modified blocking index from Lejenäs and Økland (1983). They introduced latitudinal geopotential height differences:

$$\mathrm{GHGS} = (Z(\phi_0) - Z(\phi_S))/(\phi_0 - \phi_S), \quad \text{(A1)}$$

$$\mathrm{GHGN} = (Z(\phi_N) - Z(\phi_0))/(\phi_N - \phi_0), \quad \text{(A2)}$$

with

$$\phi_N = 80°\mathrm{N} + \Delta,$$
$$\phi_0 = 60°\mathrm{N} + \Delta, \quad \text{(A3)}$$
$$\phi_S = 40°\mathrm{N} + \Delta,$$

with $\Delta = -4°, 0°, 4°$.

A longitude λ is defined as blocked on a single day if at least one Δ fulfills both of the following criteria:

$$\mathrm{GHGS} > 0 \quad \text{(A4)}$$

and

$$\mathrm{GHGN} < 10\ \mathrm{m}/°(\mathrm{lat.}). \quad \text{(A5)}$$

The second criterium was introduced to exclude situations with a far southward shifted jet zone, yet not describing blocks. With this definition time series of daily blocking indices TMI (λ) can be obtained.

For the use in this study, the blocking definition of Tibaldi and Molteni (1990) was slightly modified: according to the resolution of the grid point data Δ was changed to $\Delta = -5°, 0°, 5°$.

REFERENCES

Anonymous. 1887. Synchronous weather charts of the North Atlantic and the adjacent continents for every day from 1 August 1882, to 31 August 1883. *Q. J. Roy. Meteor. Soc.* **13**, 176–178.

Austin, J. F. 1980. The blocking of middle latitude westerly winds by planetary scale waves. *Q. J. Roy. Meteor. Soc.* **106**, 327–350.

Blackmon, M. L. and Madden, R. A. 1979. Geographical variations in the vertical structure of geopotential height fluctuations. *J. Atmos. Sci.* **36**, 2450–2466.

Boer, G. J., Arpe, K., Blackburn, M., Déqué, M., Gates, W., Hart, T. L., Le Treut, H., Röckner, E. and Sheinin, D. 1992. Some results from an intercomparisation of the climates simulated by 14 atmospheric general circulation models. *J. Geophys. Res.* **97**, **D4**, 3711–3724.

Bottomley, M., Folland, C. K., Hsiung, J., Newell, R. E. and Parker, D. E. 1990. *Global ocean surface temperature atlas.* Meteorological Office, Bracknell, 20 p. + 313 plates.

Cayan, D. R. 1992. Latent and sensible heat flux anomalies over the northern oceans: the connection to monthly atmospheric circulation. *J. Climate* **5**, 354–369.

Charney, J. G., Shukla, J. and Mo, K. C. 1981. Comparison of a barotropic blocking theory with observation. *J. Atmos. Sci.* **38**, 762–779.

D'Andrea, F., Tibaldi, S., Blackburn, M., Boer, G., Déqué, M., Dix, R. M., Dugas, B., Ferranti, L., Iwasaki, T., Kitoh, A., Pope, V., Randall, D., Roeckner, E., Straus, D., Stern, W., Van den Dool, H. and Willliamson, D. 1998. Northern Hemisphere atmospheric blocking as simulated by 15 atmospheric general circulation models in the period 1979–1988. *Climate Dyn.* **14**, 385–407.

Defant, F. 1924. Die Schwankungen der atmosphärischen Zirkulation über dem nordatlantischen Ozean im 25-jährigen Zeitraum 1881–1905. *Geografiska Annaler* **6**, 13–31 (in German).

Dole, R. M. 1978. The objective representation of blocking patterns. In: *The general circulation: theory, modeling and observations.* Notes from a Colloquium 1978, NCAR/CQ-6 + 1978-ASP, 406–426.

Dole, R. M. 1986. The life cycles of persistent anomalies and blocking over the North Pacific. In: *Anomalous atmospheric flows and blocking* (eds. Benzi, R., Saltzman, B. and Wiin-Nielsen, A. C.). *Advances in Geophys.* vol. **29**, Academic Press, New York, 31–70.

Efron, B. and Tibshirani, R. J. 1993. An Introduction to the Bootstrap. *Monographs on Statistics and Applied Probability*, vol. **57**, Chapman & Hall, New York, 436 pp.

Elliott, R. D. and Smith, T. B. 1949. A study of the effects of large blocking highs on the general circulation in the northern hemisphere westerlies. *J. Meteorol.* **6**, 67–85.

Frederiksen, J. S. 1986. Instability theory and nonlinear evolution of blocks and mature anomalies. In: *Anomalous atmospheric flows and blocking* (eds. Benzi, R., Saltzman, B. and Wiin-Nielsen, A. C.). *Advances in Geophys.* vol. **29**, Academic Press, New York, 277–304.

Glahn, H.R. 1968. Canonical correlation and its relationship to discriminant analysis and multiple regression. *J. Atmos. Sci.* **25**, 23–31.

Glowienka, R. 1985. Studies on the variability of Icelandic Low and Azores High between 1881 and 1983. *Contr. Atmos. Phys.* **58**, 160–170.

Glowienka-Hense, R. 1987. *Statistische Analyse der Nordatlantik Oszillation im Bodendruck: Beobachtung (1881–1984) und Simulation im Zirkulationsmodell T21, sowie die Rolle der Temperatur der Meeresoberflächen.* Diss. Meteorol. Inst. Univ. Bonn, 94 pp (in German).

Hense, A. 1986. Multivariate statistical investigations of the northern hemisphere circulation during the El Niño event 1982/83. *Tellus* **38A**, 189–204.

Hoffmeyer, N. 1880. N. Hoffmeyer's Studien über die Stürme des Nordatlantischen Oceans und Project eines internationalen wettertelegraphischen Dienstes in Bezug auf diesen Ocean. *Zeitschr. Österr. Ges. f. Meteorol.* **15**, 345–361 (in German).

Hoffmeyer, N. 1883. Hoffmeyer's synoptische Karten. *Zeitschr. Österr. Ges. f. Meteorol.* **18**, 252–254 (in German).

Hofmann, A. and Flohn, H. 1955. *Monatsmittel des Luftdrucks im Meeresniveau für Koordinatenschnittpunkte über dem Nordatlantischen Ozean vom Dezember 1880 bis November 1899*. DWD Scientific Rep. 1, Forschungsabteilung des DWD, Frankfurt/M., 164 pp.

Jenne, R. L. 1975. *Data sets for meteorological research.* NCAR Technical Note, IA-111, Boulder/CO, 194 pp.

Jones, P. D. 1987. The early twentieth century Arctic High — fact or fiction? *Climate Dyn.* **1**, 63–75.

Kaestner, A. 1971. Über eine Weiterentwicklung des im DWD benutzten Programms zur numerischen Analyse von Wetterkarten. *Meteorol. Rundsch.* **24**, 129–137 (in German).

Köppen, W. 1884. Tägliche synoptische Wetterkarten für den nordatlantischen Ozean und die anliegenden Theile der Kontinente. *Meteorol. Z.* **2**, 92 (in German).

Lejenäs, H. and Økland, H. 1983. Characteristics of northern hemisphere blocking as determined from a long time series of observational data. *Tellus* **35A**, 350–362.

Lejenäs, H. 1995. Long term variations of atmospheric blocking in the northern hemisphere. *J. Met. Soc. Japan* **73**, 79–89.

Liu, Q. 1994. On the definition and persistence of blocking. *Tellus* **46A**, 286–298.

Lupo, A. R., Oglesby, R. J. and Mokhov, I. I. 1997. Climatological features of blocking anticyclones: a study of Northern Hemisphere CCM1 model blocking events in present-day and double CO_2 concentration atmospheres. *Climate Dyn.* **13**, 649–666.

Mächel, H. 1995. Variabilität der Aktionszentren der bodennahen Zirkulation über dem Atlantik im Zeitraum 1881–1989. *Bonner Meteorol. Abh.* **44**, 188 pp (in German).

Makrogiannis, T. J., Bloutsos, A. A. and Giles, B. D. 1982. Zonal index and circulation change in the North Atlantic area. *J. Climatology* **2**, 159–169.

Parker, D. E., Jones, P. D., Folland, C. K. and Bevan, A. 1994. Interdecadal changes of surface temperature since the late nineteenth century. *J. Geophys. Res.* **99**, **D7**, 14,373–14,399.

Rex, D. F. 1950a. Blocking action in the middle troposphere and its effect upon regional climate: part I. *Tellus* **2**, 196–211.

Rex, D. F. 1950b. Blocking action in the middle troposphere and its effect upon regional climate: part II. *Tellus* **2**, 275–301.

Roeckner, E., Arpe, K., Bengtsson, L., Brinkop, S., Dümenil, L., Esch, M., Kirk, E., Lunkeit, F., Ponater, M., Rockel, B., Sausen, R., Schlese, U., Schubert, S. and Windelband, M. 1992. Simulation of the present-day climate with the ECHAM-Model: impact of model physics and resolution. *Max-Planck Inst. f. Meteorol. Rep.* **93**, Hamburg, 172 pp.

Römer, U. 1996. *Reaktion der Atmosphäre auf SST-Anomalien.* Diss. Meteor. Inst. Univ. Bonn, 268 pp (in German).

Rowell, D. P., Folland, C. K., Maskell, K. and Ward, M. N. 1995. Variability of summer rainfall over tropical north Africa (1906–92): observations and modelling. *Q. J. Roy. Meteor. Soc.* **121**, 669–704.

Sausen, R., König, W. and Sielmann, F. 1995. Analysis of blocking events from observations and ECHAM model simulations. *Tellus* **47A**, 421–438.

Stein, O. and Hense, A. 1994. A reconstructed time series of the number of extreme low pressure events since 1880. *Meteorol. Z., N. F.* **3**, 43–46.

Van Bebber, W. J. 1888. Synchronous weather charts of the North-Atlantic and the adjacent continents for every day from 1 August 1882 to 31 August 1883. *Meteorol. Z.* **6** (June 1888), [46].

Von Storch, H. and Zwiers, W. 1999. *Statistical analysis in climate research.* Cambridge University Press, 484 pp.

Tibaldi, S. and Molteni, F. 1990. On the operational predictability of blocking. *Tellus* **42A**, 343–365.

Tibaldi, S., D'Andrea, F., Tosi, E. and Roeckner, E. 1997. Climatology of Northern Hemisphere blocking in the ECHAM model. *Climate Dyn.* **13**, 649–666.

Treidl, R. A., Birch, E. C. and Sajecki, P. 1981. Blocking action in the northern hemisphere: a climatological study. *Atmosphere-Ocean* **19**, 1–23.

Trenberth, K. E. and Paolino, D. A. 1980. The northern hemisphere sea-level pressure data set: trends, errors and discontinuities. *Mon. Wea. Rev.* **108**, 855–872.

Walker, G. T. 1924. Correlations in seasonal variations of weather. *IX Mem. Indian Meteor. Dept.* **24**, 275–332.

Walker, G. T. and Bliss, E. W. 1932. World weather V. *Mem. Roy. Meteor. Soc.* **4**, 53–84.

Williams, J. and Van Loon, H. 1976. An examination of the northern hemisphere sea-level pressure data set. *Mon. Wea. Rev.* **104**, 1354–1361.

Woodruff, S. D., Slutz, R. J., Jenne, R. L. and Steurer, P. M. 1987. A comprehensive ocean-atmosphere data set. *Bull. Am. Meteor. Soc.* **68**, 1239–1250.